



Premixed flames propagating freely in tubes



Christophe Almarcha, Bruno Denet, Joel Quinard*

Aix Marseille Université, CNRS, Centrale Marseille, IRPHE UMR 7342, 13384 Marseille, France

ARTICLE INFO

Article history:

Received 25 June 2014

Received in revised form 17 October 2014

Accepted 21 October 2014

Available online 19 November 2014

Keywords:

Premixed flame speed

Front dynamics

Instabilities

Nonlinearity

Darrieus–Landau instability

ABSTRACT

This paper reports an experimental investigation of premixed propane and methane–air flames propagating freely downwards in tubes 1.5 m long and with diameters 54 and 94 mm. The tubes are opened at the upper end and closed at the bottom end with an acoustic damper that eliminates thermo-acoustic instability. Igniting the flame either on the tube axis or close to the wall, two regimes of propagation are distinguished by correlating the flame speed and the radius of curvature at the flame tip. The characteristic lengths are then related to the cut-off wavelengths estimated from linear theories and compared to previous results of Michelson–Sivashinsky simulations.

© 2014 The Combustion Institute. Published by Elsevier Inc. All rights reserved.

1. Introduction

The role of the hydrodynamic flame instability for premixed turbulent burning in gas turbine, spark ignition engines or industrial burners has been widely discussed [1,2]. This effect is caused by thermal expansion through the flame front and is the most essential factor in the flame instability, together with the diffusive–thermal effect that stabilizes the short-wavelength perturbations depending on the Lewis number of the deficient reactant. Now, there is a mounting evidence that the flame instability is of primary importance for turbulent burning, leading for example to an increase by a factor of 10 of the flame propagation velocity of free expanding turbulent spherical flames [3,4]. It was also suggested that this instability plays an important role in the rapid increase of U_t/U_L with pressure in high-pressure environments [5,6], where U_t/U_L is the ratio of the turbulent flame speed U_t to the laminar flame speed. Even weakly wrinkled flames maintain values of $U_t/U_L \sim 3$ –4 down to very low values of the turbulence level u'/U_L , where u' is the root-mean-square of the velocity fluctuations in the incoming gas stream [7].

These combustion instabilities are relatively well described at the onset of instability, at least for some pure fuels, and can be handled in some direct numerical simulations, but it would be a huge task to account for them in actual burners since the characteristic length scale of the flow exceeds the typical flame thickness by many orders of magnitude.

The theoretical analysis of these flames has been successful: nonlinear model equations have been derived, first by Sivashinsky in 1977 [8] and by Frankel in 1990 [9]. Simple solutions of the Sivashinsky equation have been obtained in 1985 by Thual et al. [10], and building on this discovery Joulin has studied theoretically large scale flame fronts in a number of configurations, spherical flames, oblique flames or flames of overall parabolic shape [11–14]. Numerical simulations of the Sivashinsky equation have been performed in these configurations, as they are hundred times faster than direct numerical simulations, permitting the study of very large flames [15–18]. The qualitative agreement of these simulations with experiments is excellent [19]. The observed dynamics is extremely complicated, involving cells on the flame front that continuously appear and then merge. This phenomenon possibly leads to a self-similar propagation of the flame with a fractal structure observed on free expanding spherical flames [3,4,6] or in numerical simulations [20–22]. It has been proposed [7,20–24] that weakly turbulent premixed flames also have a fractal character in other geometries. Direct numerical simulations were also performed in wide tubes with important results pertaining to the wrinkled flame speed, the onset of secondary instabilities and the flame shape (see [25–27] for an overview of DNS results in different geometries).

All these approaches refer to a characteristic length scale generally defined as the cut-off length scale λ_c due to the balance between Darrieus–Landau (DL) hydrodynamic instability and stabilizing effects of thermal diffusion. This characteristic length is the one and only parameter in theoretical models. It can be evaluated to 10–40 d_L from linear theories [28] where d_L is the laminar

* Corresponding author at: IRPHE UMR 7342, CNRS-AMU et ECM, 49 rue F. Joliot-Curie, BP 146, 13384 Marseille, France.

E-mail address: quinard@irphe.univ-mrs.fr (J. Quinard).

flame thickness, but numerical solutions of these models can hardly be compared to experimental results generally obtained in turbulent flows [7,22,29–31].

The best way for checking these models and the whole literature on the subject is to study premixed flames propagating freely in quiescent gases. The movement of a flame element will then only result from its own propagation at the normal flame speed U_L and from its advection at the local gas velocity produced by hydrodynamic effects induced by the whole flame shape. A recent experiment showed that it was possible to observe an almost stationary downwards propagation of premixed methane- and propane-air flames in tubes of various diameters, thanks to a new type of acoustic damper that eliminates the thermo-acoustic instability which otherwise would produce large acceleration effects on the flame and change drastically the flame propagation [32]. The attention was paid to the velocity of propagation of axis-symmetrical flames to be compared to self-similar relations describing free flame propagation in tubes [22,31]. The normalised wrinkled flame speed $U_n = U_t/U_L$ increased up to 2.5 while the tube diameter increases from 36 to 141 mm, and its variation with the equivalence ratio of the gas mixture was qualitatively in agreement with a self-similar relation using as cut-off wavelength the shortest unstable wavelength calculated from linear theories. The fractal exponent was close to 1/3.

Slanted flames were also observed in these experiments with a much larger propagation speed, a result not expected from Sivashinsky simulations where all solutions have the same speed and for which the more slanted flame is less stable [33]. However, faster slanted flames were also obtained when considering a flame propagating upwards without DL-instability [34] and by means of direct numerical simulation in wide tubes [22,35]. The present work aims at a better description of these two regimes of propagation by measuring simultaneously the instantaneous position of the leading flame bump and its radius of curvature. It will be shown that the flame speed is well correlated to the curvature at the leading bump. The characteristic radius of curvature at the leading bump are then related to the cut-off wavelengths and compared to the results of Michelson–Sivashinsky and numerical simulations.

2. Experimental setup and procedure

The propagation velocity of laminar cellular flames is measured in vertical Pyrex tubes, 1.5 m long, with internal diameters D_0 of 54 and 94 mm. Flames in tubes with smaller diameter would be affected by heat-losses while tubes with larger diameter can lead to a cascade of instabilities on the flame much more difficult to characterise (see Fig. 6b of Ref. [32]). Here we choose downward propagation of the flame in order to reconnect the present analysis of characteristic lengths of the flame to the results of linear theories validated at the limit of stability of planar flames [36]. Another point is that horizontal propagation would systematically lead to asymmetric flame shapes due to buoyancy effects, while upwards propagation would lead to quasi-parabolic flame shapes dominated by the dynamics of the rising bubble of hot gases [34,37].

The equivalence ratio, ϕ , of the premixed gas is controlled via a PC-interface connected to mass-flow regulators. The flame propagation is recorded using a high-speed video camera viewing the reflected images of the flame on two lines of sight at right angle (Fig. 1). The acoustic damper at the bottom part of the burner consists of a small annular slit, of height h and length l , that dissipates acoustic energy by terminating the tube with a real (resistive) acoustic impedance equal to the characteristic acoustic impedance of free air (see Ref. [32] for details). A lightweight refractory fabric is placed over the open end of the burner to prevent mixing with

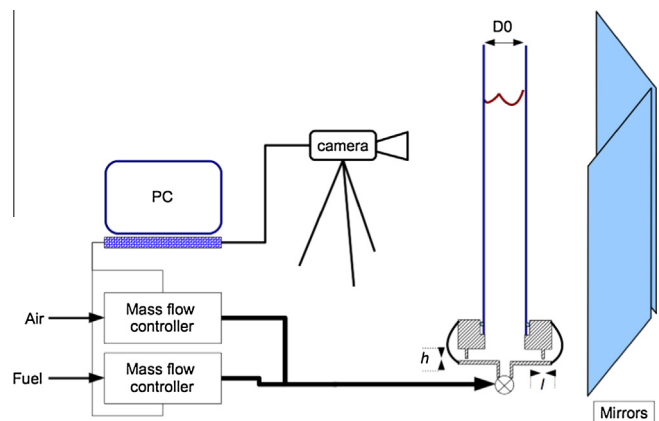


Fig. 1. Experimental set-up.

ambient air while permitting the exhaust of the premixed or burnt gas. The flame can thus propagate in an initially quiescent gas mixture without the additional effects from pressure build-up to spontaneous flame acceleration that occur in closed tubes [38].

The procedure is as follows: after each run, the air flow is opened and maintained until the tube walls have cooled to ambient temperature. The flow of combustible, methane or propane, is then adjusted to the desired equivalence ratio and maintained for a time corresponding at least to ten fillings of the tube to ensure a homogeneous mixture. Closing the valve at the bottom of the burner then stops it and a delay of at least 1 min is allowed before ignition to ensure that premixed gases are at rest. The ignition of the gas mixture is then performed by way of the fast discharge of a capacitor in a 0.1 mm radius steel wire that can be placed either on the burner axis to favour axis-symmetric flame shapes, or close to the wall to obtain slanted flames. About five runs are performed in each configuration: $\phi = (0.8, 1, 1.3)$, tube diameter = (54, 94) mm and axial or lateral ignition at the top of the burner. The video is generally recorded at a frame rate of 250 images per second. The video movies are post-processed using ImageJ 1.45r software to obtain the instantaneous position of the upstream tip of the flame and to calculate the radius of curvature in each orthogonal section of the flame (Fig. 2). The effective radius of curvature is then simply obtained by

$$2/R_f = 1/R_1 + 1/R_2$$

The mean flame speed is obtained by a linear fit of the displacement of the upstream flame tip over a distance at least equal to 0.5 m.

3. Michelson–Sivashinsky simulation

In this section, we give a brief presentation of the Michelson–Sivashinsky equation (or Sivashinsky equation, depending on the authors) that will be compared to experimental results. This equation is a model equation, which describes the non-linear behaviour of a flame submitted to a Darrieus Landau instability [8]. We will write this equation in a one-dimensional case. Let us imagine a two-dimensional premixed flame propagating towards fresh gases (at the bottom of the domain) in the y direction. The transverse coordinate will be denoted by x , and the following equation for the front position $\phi(x, t)$ can be derived (the flame laminar velocity is equal to 1, the width of the domain to 2π)

$$\phi_t + (1/2)\phi_x^2 = I(\phi) + \nu\phi_{xx} + u(x, t)$$

$I(\phi)$ is a pseudo differential operator (the Landau operator) corresponding to multiplication by $|k|$ (the wave vector) in Fourier space.

Download English Version:

<https://daneshyari.com/en/article/168752>

Download Persian Version:

<https://daneshyari.com/article/168752>

[Daneshyari.com](https://daneshyari.com)